Aquaculture Reports 45 (2025) 103205

Contents lists available at ScienceDirect

Aquaculture Reports

journal homepage: www.elsevier.com/locate/aqrep

Genome-wide association and genomic prediction of thermal tolerance in olive flounders (*Paralichthys olivaceus*): A validation study

H.M.V. Udayantha [a,b,1], Jeongeun Kim [a,b,1], Gaeun Kim [a,b], Jihun Lee [a,b], Sukkyoung Lee [a,b], Cheong-Uk Park [a,b], David B. Jones [c], Cecile Massault [c], Dean R. Jerry [c,d], D.S. Liyanage [a,b,*], Jehee Lee [a,b,*]

[a] Department of Marine Life Sciences & Center for Genomic Selection in Korean Aquaculture, Jeju National University, Jeju 63243, Republic of Korea
[b] Marine Life Research Institute, Jeju National University, Jeju 63333, Republic of Korea
[c] Centre for Sustainable Tropical Fisheries and Aquaculture, College of Science and Engineering, James Cook University, Townsville, QLD 4811, Australia
[d] Tropical Futures Institute, James Cook University, Singapore

ARTICLE INFO

Keywords:
Paralichthys olivaceus
Thermal tolerance
Single Nucleotide Polymorphism (SNP)
Marker-assisted selection
Genomic prediction

ABSTRACT

Global warming poses a significant challenge to aquaculture, with increasing water temperatures adversely affecting the growth, reproduction, and survival of aquatic species. Thus, developing thermally-tolerant strains is essential for sustaining aquaculture in a changing climate. This study aimed to identify single-nucleotide polymorphisms (SNPs) associated with thermal tolerance in olive flounders (*Paralichthys olivaceus*) and evaluate genomic prediction models for breeding thermally-resilient strains. A thermal challenge experiment was conducted with 899 fish, during which survival data were recorded under temperatures ranging from 20 ± 0.3 °C to 31 ± 0.3 °C. Genotyping using a 70 K SNP chip yielded 55,752 high-quality SNPs from 765 samples after filtering. Genome-wide association study (GWAS) identified 204 significant SNPs across eight chromosomes (chr 5, 14, 17, 18, 19, 21, 22, and 24), with annotation linking 141 genes to thermal response mechanisms. Validation in an independent population confirmed 35 common significant SNPs. Among the ten genomic prediction models tested, random forest (RF) and Bayesian B (BB) models achieved the highest prediction accuracies, with the BB model demonstrating superior reliability for estimating genomic estimated breeding values (GEBV). Further, cross-validation indicated that most fish with high GEBV survived the thermal challenge. These findings underscore the potential of genomic prediction in developing thermally-tolerant olive flounder strains, offering a robust strategy to enhance aquaculture sustainability amid ongoing climate change.

1. Introduction

Olive flounder (*Paralichthys olivaceus*) is an economically important marine fish species widely distributed along the coastlines of East Asia, particularly in China, Japan, and Korea. These flatfish are extensively cultured for commercial purposes owing to their high market demand and notable traits, including rapid growth, high flesh quality, and adaptability to diverse environmental conditions (Lee et al., 2022; Stieglitz et al., 2021; Zeng et al., 2019). The Republic of Korea is the largest global producer of farm-raised olive flounder, with an output of 45,884 tons in 2022, representing over 53 % of the total cultured fish production of the nation (Statistics Korea, 2022). More than half of this production is attributed to aquaculture operations on Jeju Island. Despite their economic importance, the sustainability and productivity of olive flounder aquaculture are increasingly threatened by environmental stressors, including rising sea temperatures associated with global warming (Han et al., 2024; Maulu et al., 2021; Yazdi and Shakouri, 2010).

Thermal tolerance (TT), defined as the ability of an organism to withstand elevated temperatures, is a crucial trait influencing the performance, survival, and overall health of aquatic species, particularly that of cold-blooded animals (Alfonso et al., 2021; Pandit and Nakamura, 1970). Optimal culturing temperatures for olive flounders range from 19 to 23 ℃ (Jung et al., 2020), whereas their maximum tolerance is under 32.5 ℃ (Udayantha et al., 2023). However, increasing water temperatures in South Korean seas have resulted in consistently

* Correspondence to. Marine Molecular Genetics Lab, Jeju National University, 102 Jejudaehakno, Jeju 63243, Republic of Korea.
E-mail addresses: dileepa@jejunu.ac.kr (D.S. Liyanage), jehee@jejunu.ac.kr (J. Lee).
[1] These authors contributed equally to this work

https://doi.org/10.1016/j.aqrep.2025.103205
Received 30 April 2025; Received in revised form 13 September 2025; Accepted 28 October 2025
Available online 7 November 2025

increasing flounder mortality from 2018 to 2022 (Lee, 2024). Thus, understanding the genetic basis of TT in olive flounder is essential for developing resilient broodstocks and ensuring the sustainability of aquaculture operations amid climate variability.

Genome-Wide Association Studies (GWAS) are powerful tools for elucidating the genetic architecture of complex traits, such as TT, in non-model species, such as olive flounder. GWAS analysis identifies genetic variants associated with phenotypic variation by scanning the entire genome. In contrast, genomic prediction uses genome-wide marker information to estimate breeding values for these traits, without necessarily identifying specific causal variants, thereby facilitating the selection of superior candidates for breeding programs (Li et al., 2017; Meuwissen et al., 2001).

Recent studies have applied these approaches to explore the genetic basis of various traits in aquatic species, such as resistance to nervous necrosis virus in *Dicentrarchus labrax* (Palaiokostas et al., 2018), feed conversion efficiency in *Oreochromis niloticus* (Barría et al., 2021), growth in *Clarias macrocephalus* (Chaivichoo et al., 2023), fillet yield in *Oncorhynchus mykiss* (Garcia et al., 2023), sea lice in *Salmo salar* (Garcia et al., 2024), resistance to Viral hemorrhagic septicemia virus (VHSV) and growth in *P. olivaceus* (Liyanage et al., 2022; Omeka et al., 2022), and TT in *Haliotis discus hannai* (Liu et al., 2022).

While previous studies have explored the genetic architecture of TT in olive flounder, comprehensive validation studies that integrate both GWAS and diverse genomic prediction models, alongside cross-population evaluation, remain limited. This study addresses this gap by providing a systematic validation of genomic tools for predicting TT in olive flounder. Specifically, we validated significant SNPs by testing their consistency in an independent olive flounder population (dF0) and further evaluated the predictive performance of genomic models through within-population cross-validation and cross-population prediction analyses.

2. Materials and methods

2.1. Olive flounder rearing, thermal challenge, and fin clipping

The dF0 generation used in the TT experiments was produced through artificial mating at a hatchery in Jeju, South Korea. A total of 204 dams and 86 sires, previously genotyped using a 70 K SNP array, were used to generate 164 full- and half-sib families. Parentage assignment revealed that 57 dams and 62 sires contributed to the current study population. The parent candidates were kept in a flow-through aquaculture system at the Haeyeon fishery in Jeju Island. Fish were fed with moisture pellets at a rate of 2.1 % body weight per day, and the water temperature, dissolved oxygen level, and salinity were 17.1 ± 0.1 ℃, 7.0 ± 0.5 mg/L, and 33.5 ± 0.9 PSU, respectively, during sexual maturation. Each family consisted of approximately 1–34 individuals. Fertilized eggs were incubated, and larvae were reared in underground seawater maintained at 20 °C and 33.5 PSU salinity. Larvae were initially fed rotifers and artemia for 35 days, followed by a transition to commercial feed until the start of the thermal challenge experiment. To understand the genetic background of the dF0 population, parentage assignment was performed using SNP markers, confirming the family structure. A total of 899 healthy, ten-month-old dF0 olive flounders (total length = 26.0 ± 2.2 cm; mean weight = 172.7 ± 44.1 g) were transferred to four tanks at the Ocean and Fisheries Research Institute, Pyoseon-myeon, Jeju Special Self-Governing Province, Republic of Korea. Prior to the experiment, the fish were acclimatized for one week in recirculating aquaculture systems at 20.0 ± 0.2 ℃, with dissolved oxygen (DO) levels maintained at ≥ 120 %. The thermal challenge consisted of a gradual increase in water temperature over 18 d (Fig. 1). The temperature was increased by 1 ℃ per day for 10 d, reaching 30.0 ± 0.3 ℃. Subsequently, the temperature was raised to 30.5 ± 0.3 ℃ and maintained for 3 d, followed by an increase to 31.0 ± 0.3 ℃ for the remaining 5 d. Fish that survived the 18-d challenge were categorized as thermally tolerant. During the thermal challenge, fish were monitored at 30-min intervals. Fish that were observed dead were promptly removed, and a fin clip was collected for subsequent DNA extraction. For the surviving fish, fin clipping was performed at experiment termination. Fin samples were stored at -80 ℃ until genomic DNA (gDNA) extraction. Morphometric data, including total length, width, and weight, as well as tank information and survival data, were recorded for all fish. Additionally, three survival traits were defined for further analysis: binary survival (SUR), days to death based on the date of death (DPC_Date), and days to death based on the time of death (DPC_Time). The dF0 validation population, consisting of 768 individuals, was phenotyped for TT using the same experimental design and data collection protocol as the nF0 population. Complete details of the nF0 thermal challenge are described in Udayantha et al. (2023). This study followed the guidelines of the Animal Experiment Ethics Committee of Jeju National University.

2.2. 70 K SNP array design

A total of 103 broodstock fish from the same breeding facility (unrelated to the dF0 and nF0 populations used in this study) were subjected to whole-genome re-sequencing for SNP discovery and high-confidence variant selection for SNP array design (not yet commercially available). Briefly, approximately 401.81 million raw SNPs were initially called using GATK after mapping to the reference genome (ParOli_1.1; GCA_001904815.2). Filtering by MAF ≥ 0.05, genotyping rate ≥ 0.1, and HWE ≥ 0.001 reduced this to 154,964 candidate SNPs, which were evaluated using Affymetrix pConvert scores, with A/T and C/G SNPs deprioritized, resulting in ~70,000 SNPs passing final QC for inclusion in the array. Complete details of array design and probe construction are described in Liyanage et al., (2022) (Liyanage et al., 2022).

2.3. Genotyping and quality control (QC)

Fin samples (approximately 50–60 mg) from 899 individuals, preserved at -80 ℃, were treated with absolute ethanol and sent to BluGen (Busan, Republic of Korea) for gDNA extraction and genotyping. Genotyping was performed using the 70 K SNP Affymetrix® Axiom® myDesign™ Genotyping Array (custom-design, unpublished). Although 899 samples were originally phenotyped for TT, genotyping was successfully completed for only 768 samples. The remaining 131 samples

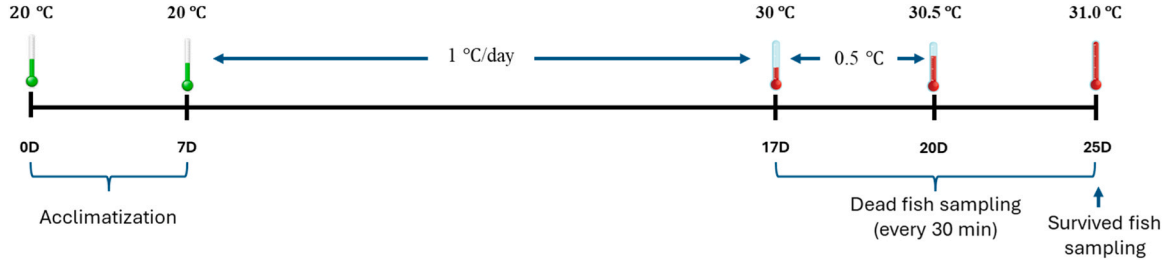

Fig. 1. Schematic representation of sampling technique.

were excluded due to insufficient tissue material, degraded DNA quality, or failure to meet minimum genotyping requirements. Following genotyping, quality filtering was performed according to a previously established protocol (Liyanage et al., 2022). The raw genotyping data was first pre-processed using the Axiom Analysis Suite, where SNPs were filtered using the "PolyHighResolution" setting to remove markers with poor clustering quality. Initial filtering with PLINK 1.9 identified 56,455 SNPs across 24 chromosomes from 765 fish samples (3 samples failed during QC). Additional QC steps were performed using PLINK 1.9, applying the following criteria: MAF ($\geq$ 0.05), HWE ($\geq$ 0.01), and genotyping rate ($\geq$ 0.1). These steps produced a final dataset of 55,752 high-quality SNPs for subsequent analyses.

2.4. Identification of population structure

The genetic structure of the population was assessed using principal component analysis (PCA) and a genomic relationship matrix (GRM). PCA plots were generated to visualize genetic clustering among individuals, and k-means clustering was applied to identify subpopulations based on PCA results. SNP data from 765 individuals (after QC filtering) were used to visualize population structure. PCA results were visualized using the ggplot2 package in R. K-means clustering was then performed on the first 10 principal components using the kmeans() function in R, and the optimal number of clusters (K = 4) was determined based on the number of populations identified by the scree plot. The distribution of families across the population was also assessed.

2.5. Heritability, GWAS, and validation

Prior to the association analysis, the distribution of the phenotypes was assessed, and normality testing was performed to ensure that the data fit the assumptions of the linear mixed model used for GWAS. Narrow-sense heritability (h^2) for the traits SUR, DPC_Date, and DPC_Time was estimated using the GCTA package (Yang et al., 2011) with the following equation:

$$h^2 = \frac{\sigma_A^2}{\sigma_A^2 + \sigma_E^2},$$

where σ_A^2 denotes the additive genetic variance and σ_E^2 represents the residual variance.

Variance components were estimated using the Average Information Restricted Maximum Likelihood (AI-REML) algorithm in GCTA with the following linear mixed model:

$y = Xb + Zu + e$,

where:

y = is the vector of phenotypic observation (measured as time-to-death),

b = is the vector of fixed effects and covariates, which includes:

- tank effect (to account for environmental differences),
- body weight, total length, and total width (morphometric traits as covariates),
- the first ten principal components (PC1–PC10) from PCA (to correct for population structure),

X = is the incidence matrix for fixed effects and covariates,

u = is the vector of random additive genetic effects, assumed to follow $u \sim N(0, G\sigma_g^2)$

Z = incidence matrix relating phenotypes to individuals,

e =is the vector of residual errors, assumed $e \sim N(0, I\sigma_e^2)$, and

G = is the genomic relationship matrix (GRM) derived from SNP data.

Manhattan and quantile-quantile (QQ) plots were generated using the qqman and CMplot packages in RStudio. Genome-wide significance was determined using a conservative Bonferroni correction threshold of $p < 1 \times 10^{-8}$, which is more stringent than the nominal 0.05/55,752 $\approx 8.96 \times 10^{-7}$ cutoff, to minimize false positives due to the small sample size and population structure (Forutan et al., 2024; Mesbah-Uddin et al., 2022). Suggestive associations were defined at $p < 1 \times 10^{-5}$.

Genomic correlations among traits (SUR, DPC_Date, DPC_Time, Weight, Length, and Width) were estimated using a multivariate linear mixed model implemented with the lmm.diago function in the Gaston package R. This model leverages the genomic relationship matrix (G) to estimate additive genetic (co)variances, providing robust estimates of genomic correlations between traits while accounting for population structure and genetic relatedness among individuals. Validation of significant SNPs was performed by conducting an independent GWAS for TT in the nF0 population (nF0_TT), which included 58,920 high-quality SNPs from 768 individuals (Udayantha et al., 2023), using the same SNP array and analysis pipeline as the dF0 population. SNPs that were significantly associated in both dF0 and nF0 populations were considered validated. Additionally, bar plots comparing significant SNP associations between the current dF0 population and the nF0_TT population were generated using the ggplot2 package in R.

2.6. Significant SNPs and functional annotation

Significant SNPs identified from GWAS were annotated based on their physical positions in the olive flounder genome to identify nearby or overlapping genes. Annotation was performed using the olive flounder genome assembly (ParOli_1.1; GenBank assembly GCA_001904815.2). These SNPs, along with their adjacent nucleotide sequences, were then manually annotated using the National Center for Biotechnology Information (NCBI) Basic Local Alignment Search Tool (BLAST) to identify related protein sequences and infer potential functional roles.

2.7. k-fold cross-validation using different prediction algorithms

For genomic prediction analysis, the QC-filtered dataset containing 55,752 SNPs from 765 samples and their phenotypic data (described in Section 2.3) was utilized. Ten genomic prediction models were evaluated to identify the most accurate model for predicting the dF0 TT (dF0_TT) trait. These models included one penalized approach (Genomic Best Linear Unbiased Prediction (GBLUP)), five Bayesian models (Bayesian A (BA), Bayesian B (BB), Bayesian C (BC), Bayesian Lasso (BL), and Bayesian ridge regression (BRR)), and four machine learning models (ridge regression (RR), elastic net (EN), reproductive kernel Hilbert space (RKHS), and random forest regression (RF)).

Prior to analysis, SNP data were converted to numerical genotypes (-1 for homozygous AA, 0 for heterozygous AB, and 1 for homozygous BB). GBLUP assumes that all SNPs contribute equally by assigning them the same variance. Bayesian models allow for variable SNP effects, including some with zero contribution. EN applies a combination of L1 (lasso) and L2 (ridge) regularization to handle multicollinearity and variable selection. RF captures complex, non-linear interactions among SNPs through tree-based ensemble learning. RKHS models non-linear genetic relationships using kernel matrices, allowing for flexible modeling of additive and epistatic effects. All models were implemented using the BGLR, randomforest, or glmnet packages with default hyperparameters optimized by internal grid search. Additionally, the summary of models is categorized in Table 1. A 3-fold cross-validation replicated 10 times (30 total runs) was used to balance the training/validation ratio in our dataset, and the mean accuracy with standard deviation was reported. Moreover, prediction accuracy was calculated as the Pearson correlation between observed phenotypes and predicted genomic breeding values in the validation set. Prediction bias was evaluated as the regression coefficient of observed phenotypes on predicted GEBVs. One-way analysis of variance was applied to assess significant differences among models for each trait, followed by Tukey's

Table 1
Summary of genomic prediction models used in this study, including their statistical nature, key assumptions regarding genetic architecture, ability to capture non-linear effects, and the software packages used for implementation.

Model	Nature	Key Assumption	Captures Non-linear Effects?	Software
GBLUP	Linear	Equal SNP variance	No	BGLR
Bayesian models	Bayesian	Some SNPs have 0 effect	No	BGLR
EN	Penalized regression	Combines L1/L2 regularization	No	glmnet
RF	Machine learning	Tree-based bagging	Yes	caret
RKHS	Kernel-based	Gaussian kernel for SNP similarity	Yes	BGLR

honest significant difference test for post hoc multiple comparisons using RStudio.

Comprehensive details of each model are listed below: GBLUP, a widely used model, assumes all SNPs contribute equally to genetic variance (Fernando and Grossman, 1989). GEBVs were calculated using the equation:

$$Y = Zg + X\beta + e,$$

where Y is the phenotypic vector, Z is the incidence matrix for fixed effects, X is the incidence matrix for random effects, g is the vector of random effects, β is the vector of fixed effects, and e is the residual effect. It was assumed that $e \sim N(0, I\sigma_e^2)$ and $g \sim N(0, K\sigma_g^2)$, where I is the identity matrix, and K is the genomic relatedness matrix.

All Bayesian models (BA, BB, BC, BL, and BRR) follow a general form with minor modifications (Habier et al., 2011; Park and Casella, 2008) and were implemented using the BGLR statistical package (Pérez and de los Campos, 2014):

$$Y = X\beta + \sum_{k=1}^{K} z_k \alpha_k + e,$$

where Y, X, β, and e are as defined for GBLUP. α_k represents the vector of random effects for the k^{th} SNP, and z_k is the vector of genotypes at the k^{th} SNP. The models differ in their prior distributions for SNP effects: BA assumes normal distribution with variances set to one for all SNPs; BB sets SNPs variances to zero with an inverted chi-square distribution; BL assumes a Laplace distribution for SNP variances; and BRR applies a Gaussian prior, where all effects shrink similarly.

RR addresses multicollinearity in linear regression by adding a penalty term to the size of the coefficients (Ogutu et al., 2012). Briefly, in the context of genomic prediction, the design matrix X includes SNP genotypes coded as 0, 1, or 2, representing the number of reference alleles per individual. The regularization parameter λ, which controls the degree of shrinkage, is defined as the ratio of the residual variance to the prior variance of SNP effects (σ_β^2), typically estimated via restricted maximum likelihood (REML). The model is defined as:

$$\|y - X\beta\|^2 + \lambda\|\beta\|^2,$$

EN combines lasso and ridge regression (Ogutu et al., 2012) and is formulated as:

$$\|y - X\beta\|^2 + \lambda_1\|\beta\|_1 + \lambda_2\|\beta\|^2,$$

In the EN model, the design matrix X contained SNP genotypes coded as 0, 1, or 2. The model minimizes the objective function $||y - X\beta||2 + \lambda1||\beta||1 + \lambda2||\beta||22$, where $\lambda1 = \alpha\lambda$ and $\lambda2 = (1 - \alpha)\lambda$. The overall penalty λ and the mixing parameter α were optimized by internal 10-fold cross-validation within each training set using the cv.glmnet() function, selecting the λ that minimized mean squared error.

RKHS uses kernel functions to map data into higher dimensions, capturing non-linear relationships (Gianola and van Kaam, 2008) and is defined as:

$$f(x) = \sum_{i=1}^{n} \alpha_i K(x, x_i),$$

where $f(x)$ is the estimated regression function, α_i are coefficients, and $K(x, x_i)$ is the kernel function that measures similarity between input x and training data point x_i.

Finally, RF constructs multiple decision trees and averages their predictions to improve accuracy and reduce overfitting (Breiman, 2001). The model is represented as:

$$\hat{y} = \frac{1}{N}\Sigma_i^N = 1^T \hat{\imath}(x),$$

For the RF model, we used 500 decision trees (ntree = 500), the standard default value for the R package, which is widely considered a robust choice for balancing model performance and computational efficiency.

2.8. Prediction accuracy by population size

The influence of population size on prediction accuracy was examined using the GBLUP and BB models. These models were selected due to their ability to incorporate fixed effects, which enhances prediction accuracy. Moreover, BB achieved the highest accuracy among Bayesian models in our evaluations. Notably, GBLUP is a widely adopted genomic prediction model that assumes an infinitesimal genetic architecture (Hayes et al., 2009; Lee et al., 2023), whereas BB assumes a sparse architecture where only a subset of SNPs have large effects. Therefore, these two models were chosen as complementary benchmarks to represent the two main extremes of genetic architecture assumptions. For the population size effect analysis, we randomly sampled different training population sizes (25, 50, 100, 200, 300, 400, 500, 600, and 765 individuals) from the full dataset. For each training size, 10 independent random samples were generated. The remaining individuals not included in the training set served as the validation population. The model (GBLUP or BB) was fitted on the sampled training set, EBVs were predicted for the validation set, and prediction accuracy was calculated. The final accuracy for each training size was reported as the mean ± SD across 10 replicates. Prediction bias was evaluated as the regression coefficient of observed phenotypes on predicted GEBVs. A coefficient value approaching 1.0 indicates that the prediction is unbiased, while values deviating from 1.0 suggest either overestimation (>1) or underestimation (<1) of breeding values.

2.9. Prediction accuracy by marker density

The influence of marker density on prediction accuracy was assessed using the GBLUP and BB models. For SNP density analysis, SNPs were randomly sampled from the QC-confirmed markers to create different density levels, such as 100, 500, 1000, 5000, 10,000, 20,000, 30,000, 40,000, 50,000, and 56,000. For each density level, 10 independent random SNP subsets were generated. Prediction accuracy was evaluated using the same 3-fold cross-validation replicated 10 times as described in Section 2.7, and the mean ± SD across replicates was reported, and prediction bias was calculated. All 765 individuals from the dF0_TT datasets were included in the analysis.

2.10. Prediction cross-validation with nF0 population

For cross-population prediction, the intersection of SNPs common between dF0_TT (55,752 SNPs) and nF0_TT (58,920 SNPs) was used, resulting in 55,752 markers. The prediction model was trained on dF0_TT and applied to nF0_TT, for which thermal tolerance phenotypes were available. Prediction accuracy was calculated as the Pearson correlation between phenotypes and predicted GEBVs. We then compared the cross-population prediction accuracy (dF0_TT → nF0_TT) with the

within-population accuracy previously obtained from 3-fold cross-validation (10 replicates) in dF0_TT.

3. Results

3.1. Thermal challenge assay and sample collection

The thermal challenge assay consisted of 899 olive flounders, of which 829 fish died and 70 survived, resulting in a cumulative mortality rate of 91.6 % (Fig. 2). The highest mortality occurred on day 12, coinciding with the peak water temperature of 30.5 °C, during which 459 fish died. Additionally, the family status and summary statistics of the experimental population are provided in Supplementary Figures 1–4 and Supplementary File 1.

3.2. QC filtering

After genotyping, 765 individuals passed quality control filtering. Following probe filtering and additional QC thresholds, a total of 55,752 high-quality SNPs were retained for downstream analyses.

3.3. Population distribution and heritability

The first two principal components explained 11.96 % and 10.63 % of the population structure and genetic relatedness, respectively (Fig. 3 A, 3B, and 3 C). Collectively, the first 10 principal components explained approximately 68.17 % of the total population variance. Survival rates varied across subpopulations: subpopulations 1, 2, 3, and 4 exhibited survival rates of 8.99 %, 4.14 %, 0.91 %, and 15.45 %, respectively.

The heritability for survival (SUR) was 0.39 ± 0.05, whereas heritabilities for days to death based on date (DPC_Date) and time (DPC_Time) were 0.72 ± 0.04 and 0.74 ± 0.04, respectively (Table 2).

Further, we analyzed phenotypic and genotypic correlations among traits (SUR, DPC_Date, DPC_Time, weight, length, and width) (Fig. 4). Phenotypic correlations showed a strong positive correlation (0.65 ± 0.03) between survival and both DPC_Date and DPC_Time, with an almost perfect correlation (0.99 ± 0.01) between DPC_Date and DPC_Time. This strong correlation is expected because Time represents a finer-scale measurement of the same event, where Date can be predicted directly from the time of death (e.g., <24 h = day 1, 24–48 h = day 2). Therefore, we focused on Time as the primary phenotype for downstream analyses, as it provides greater phenotypic resolution and variability, which is advantageous for GWAS and genomic prediction. Negative correlations were observed between weight, length, and width with survival, DPC_Date, and DPC_Time (Fig. 4). Genotypic correlations showed a similar trend: survival exhibited a positive correlation of 0.62 ± 0.03 with both DPC_Date and DPC_Time, and the correlation between DPC_Date and DPC_Time was 0.9 ± 0.02 (Fig. 4).

3.4. Genome-wide association analysis and validation

A total of 204 significant SNPs were identified across the three analyzed traits: seven for binary survival, 198 for DPC_Date, and 204 for DPC_Time (Fig. 5 A, 5B, and 5 C). These SNPs were distributed across eight chromosomes: chr 5 (2 SNPs), chr 14 (1 SNP), chr 17 (2 SNPs), chr 18 (53 SNPs), chr 19 (145 SNPs), chr 21 (2 SNPs), chr 22 (1 SNP), and chr 24 (4 SNPs). Notably, all seven significant SNPs identified for DPC_SUR were also common to all three traits. These SNPs were AX-419312234, AX-419312236, AX-419194958, AX-419285141, AX-419194938, AX-419197087, and AX-419197637. Further, complete GWAS summary statistics of three traits, including SNP_ID, chromosome position (POS), allelic substitution effect with standard error (SE), and *p*-value for all tested SNPs, are provided in Supplementary File 2.

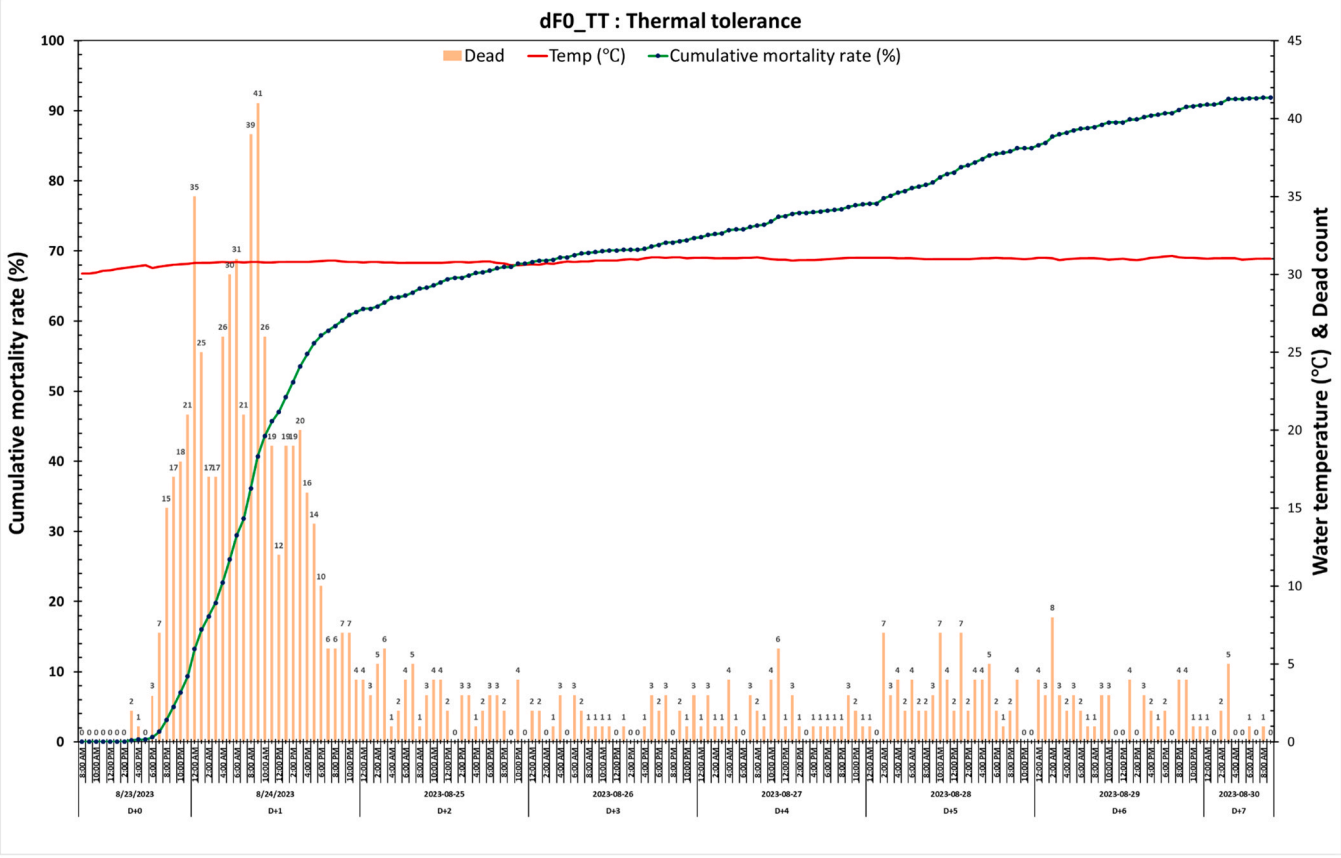

Fig. 2. Cumulative mortality and temperature fluctuations of the thermal challenge experiment (starting from the first dead).

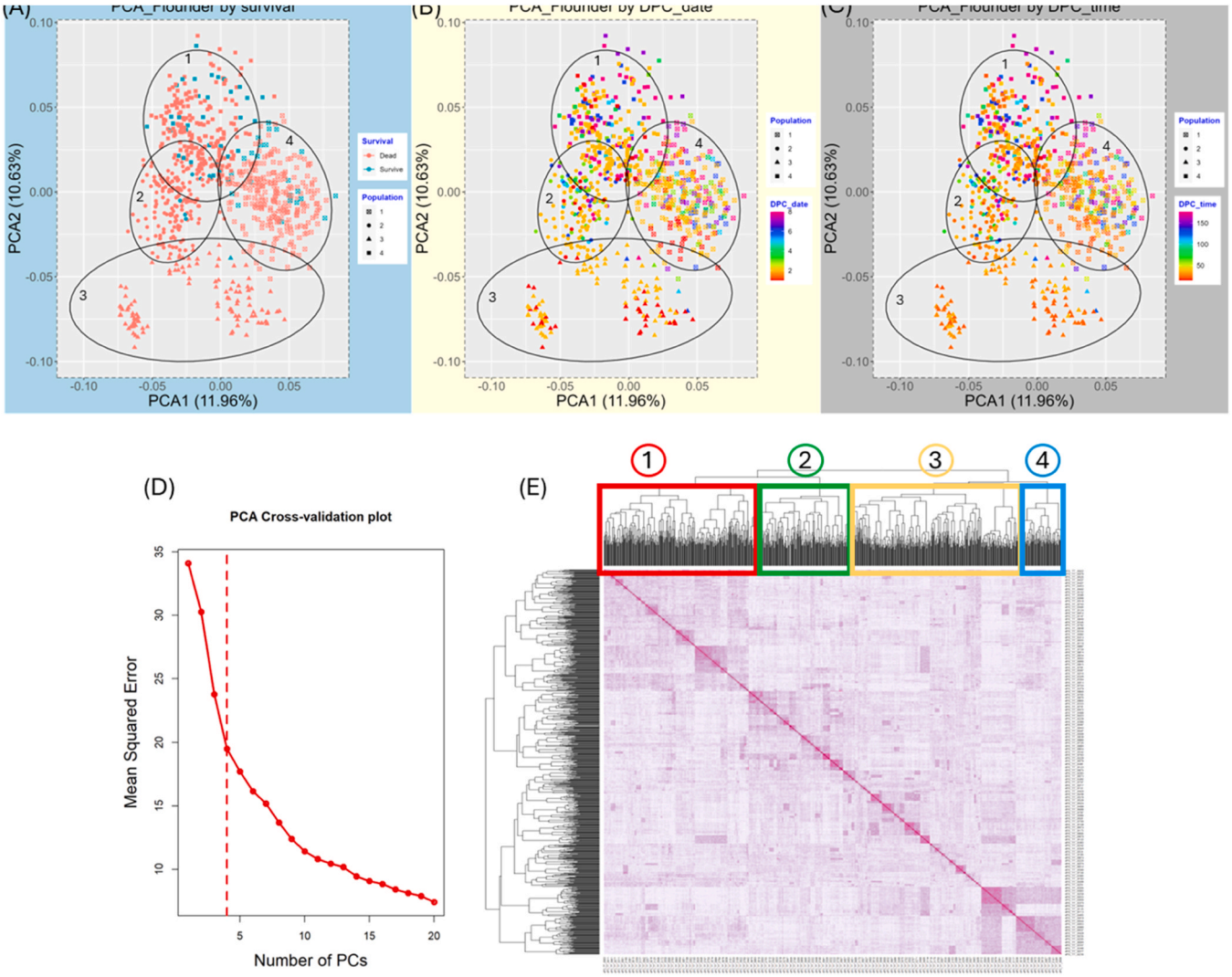

Fig. 3. Population stratification of the olive flounder in the study population. (A, B, C) Principal component analysis (PCA) of binary survival (SUR), DPC_Date, and DPC_time, respectively. Subpopulations represented in the study population are denoted as 1–4. (D) Scree plot of the PCA. The vertical red dashed line denoted the four subpopulations in the study population and (E) Heat map of the Genomic Relationship Matrix (GRM). Red, green, yellow, and light blue boxes represent the subpopulations in the study population.

Table 2
Heritability and genetic variance for thermal tolerance traits in the olive flounder.
Superscripted slowercase letters denote the significant difference ($p < 0.05$) among traits.

Phenotypic trait	Genetic variance (Vg)	Residual variance (Ve)	Phenotypic variance (Vp)	Heritability (h^2)
SUR	0.03 ± 0.005	0.05 ± 0.004	0.08 ± 0.005	0.39 ± 0.05[a]
DPC_Date	3.38 ± 0.4	1.34 ± 0.1	4.72 ± 0.3	0.72 ± 0.04[b]
DPC_time	1956.17 ± 237.6	698.55 ± 76.3	2654.72 ± 200.9	0.74 ± 0.04[b]

The identified SNPs were distributed across various genomic regions: 20 in exons, 84 in introns, and 98 in intergenic regions. The QQ plots showed a slightly left-skewed pattern, with λ values < 1, indicating a conservative genomic control and minimal inflation of test statistics. Additionally, the calculated λ values were 0.494 for SUR, 0.302 for DPC_Date, and 0.296 for DPC_Time.

A total of 35 SNPs were found to be significantly associated with TT in both populations. The complete list of these SNPs, along with their summary statistics in each population, is provided in Supplementary File 3. Functional annotation of these SNPs revealed associations with 27 genes (Table 3). Among the 35 common SNPs, several were located within the same gene regions, resulting in fewer unique genes than the total number of significant SNPs. For example, AX-419194853, AX-419197072, and AX-419310932 are all located within or near the gene ST3 beta-galactoside alpha-2,3-sialyltransferase 2. Among the top 10 most significant SNPs in each population, five were shared: AX-419312234, AX-419312236, AX-419197087, AX-419194856, and AX-419312238. These shared SNPs exhibited consistent distribution patterns in both populations (Fig. 6A and 6B), although PCA indicated differing overall population structures between the dF0 and nF0 populations (Fig. 6C). Additionally, the genetic relationship between the dF0 and nF0 is shown in Supplementary Figure 5.

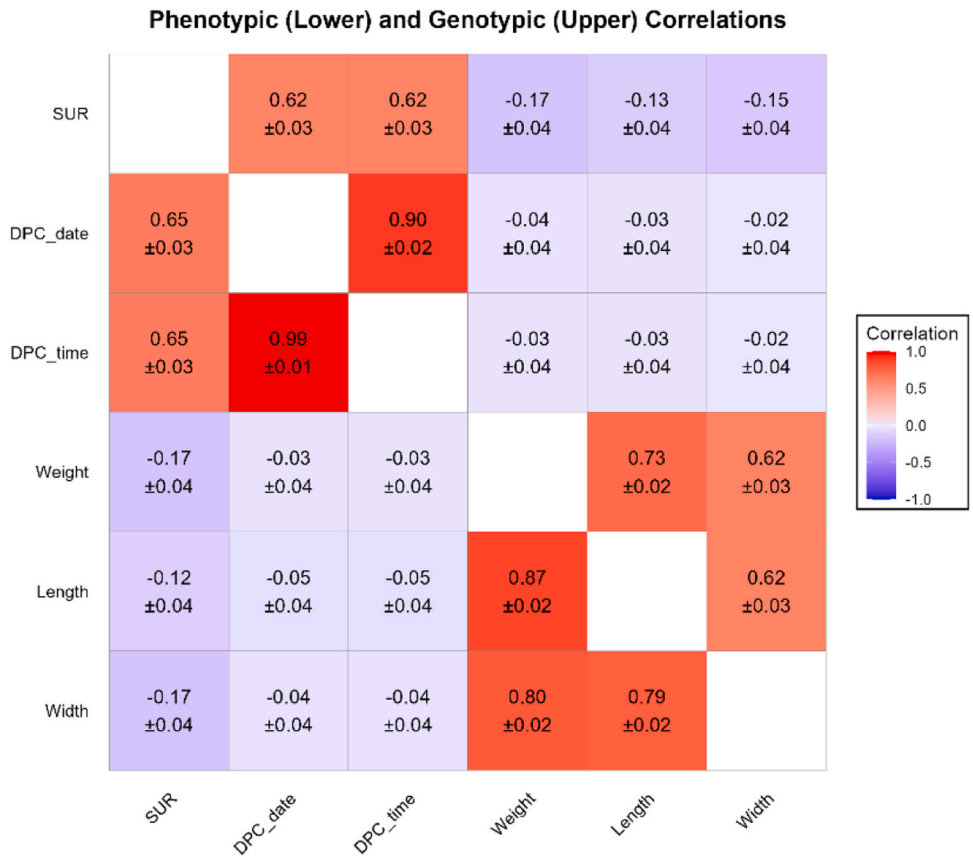

Fig. 4. Heat map of phenotypic and genotypic correlations of five traits (SUR, DPC_Date, DPC_time, Weight, Length, and Width) with standard error (SE).

3.5. SNP and functional annotation

The 204 significant SNPs identified through GWAS were annotated against the *P. olivaceus* reference genome to identify associated genes and predict their biological functions, which identified 141 putative functional genes. Of these, 29 genes were associated with multiple SNPs (accounting for 90 SNPs), whereas 112 genes were linked to a single SNP each. Two SNPs were not located within or in proximity to any annotated genes. The complete list of genes, associated SNPs, and details of the SNPs are provided in Supplementary File 4.

3.6. Comparison of different genomic prediction models

The random forest (RF) model consistently exhibited the highest prediction accuracy for all traits. For SUR, prediction accuracies ranged from 0.41 to 0.53, with RF, RKHS, and GBLUP demonstrating the highest accuracies, while the BA model yielded the lowest accuracy (Fig. 7A and Table 4). Notably, RF outperformed all other models with statistically significant differences (Supplementary File 5). For DPC_Date, accuracies ranged from 0.68 to 0.84, with RF, BB, and EN models achieving the highest performance, while the RR model had the lowest performance (Fig. 7B). A similar trend was observed for DPC_Time, with accuracies ranging from 0.68 to 0.84 (Fig. 7C and Table 4). Consistently, the RF model significantly outperformed all other prediction models for both DPC_Date and DPC_Time (Supplementary File 5). The mean accuracy and bias of each model are provided in Supplementary Table 1.

3.7. Effect of population size on prediction accuracy

Population size had a significant effect on prediction accuracy, with smaller sizes resulting in lower accuracy and larger sizes improving accuracy (Fig. 8). For the BB model, prediction accuracies exceeded 0.70 for DPC_Date and DPC_Time when the population size reached 200 and further improved with increasing training population size, but the rate of improvement slowed beyond ~200 individuals, indicating diminishing returns rather than a complete plateau (Fig. 8B, C). For SUR, accuracy improved to over 0.40 when the population size reached 500 (Fig. 8A). Based on these results, prediction accuracy improved with increasing training population size for both BB and GBLUP models. For the BB model, accuracy gains became smaller beyond ~200 individuals for DPC_Date and DPC_Time, whereas SUR required around 500 individuals to reach comparable accuracy levels. For the GBLUP model, accuracies for DPC_Date and DPC_Time exceeded 0.60 at a population size of 400, while SUR reached 0.40 at the same sample size (Fig. 8D–F). However, no complete plateau was observed, and further increases in sample size are expected to continue improving prediction accuracy as the population size increases. Supplementary Table 2 presents the calculated mean accuracy and bias values for each population size.

3.8. Effect of SNP density on prediction accuracy

Based on our results, prediction accuracy improved with increasing SNP density, but the rate of improvement diminished beyond ~5000 SNPs for SUR and ~10,000 SNPs for DPC_Date and DPC_Time with the BB model (Fig. 9A–C). Similarly, in GBLUP, accuracies exceeded 0.65 with ~5000 SNPs, after which only marginal gains were observed for both traits (DPC_Date and DPC_Time) (Fig. 9E and F). These results suggest that while higher SNP densities continue to improve accuracy, the benefit becomes less pronounced beyond 5000–10,000 SNPs. Supplementary Table 3 summarizes the mean accuracy and bias for each SNP number.

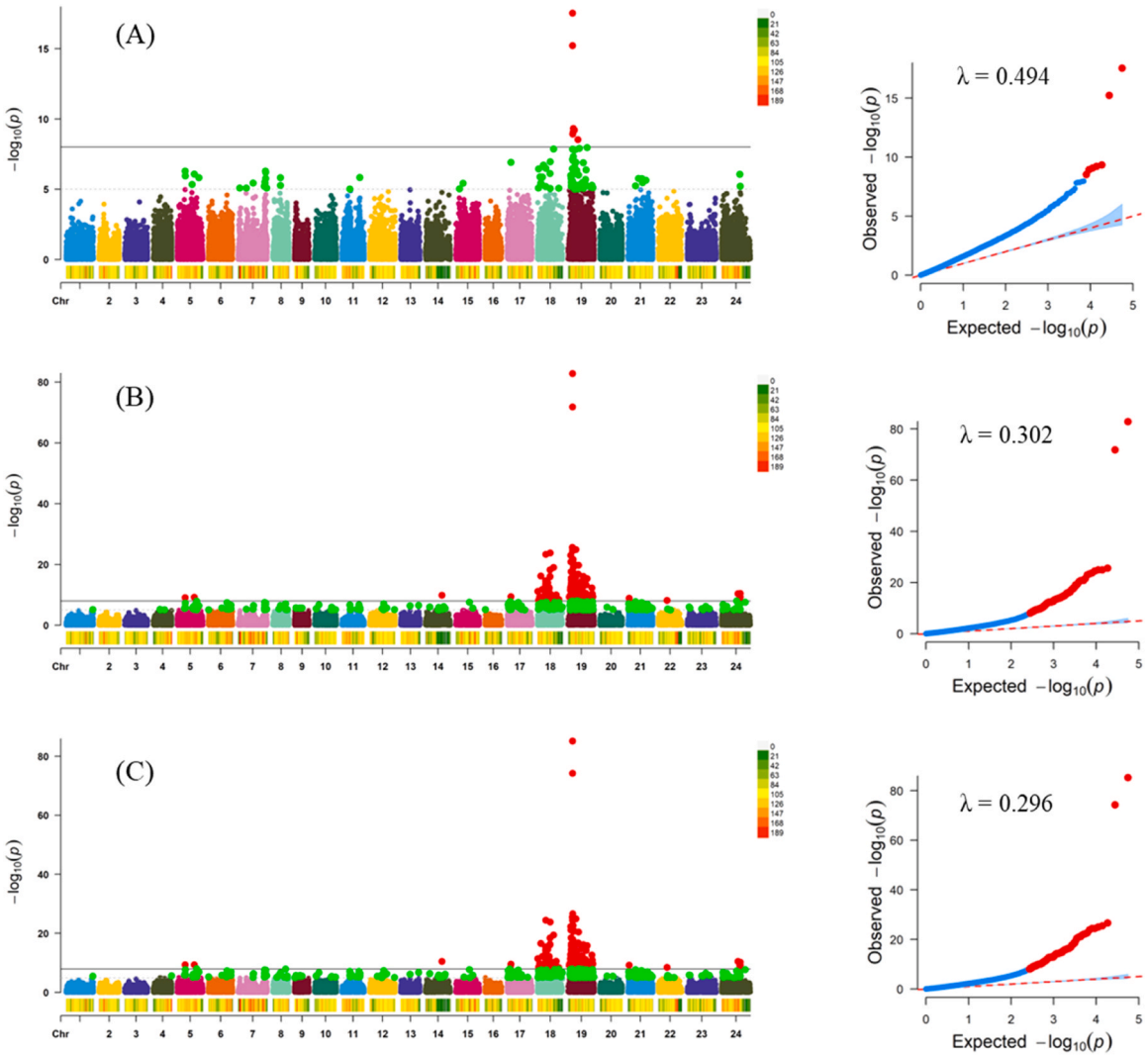

Fig. 5. Manhattan and QQ plot of GWAS analysis. A, B, and C represent the survival, DPC_Date and DPC_Time, respectively. Genome-wide association (1 x 10^{-8}) and suggestive association (1 x 10^{-5}) are represented in the black and dotted lines respectively. In QQ plots, the lambda (λ) represents the genomic inflation factor values of GWAS.

3.9. Cross-population genomic prediction

While genomic prediction in aquaculture breeding programs is typically applied within families or among closely related individuals, where relationships between training and validation populations strongly influence accuracy, our cross-population analysis was conducted as an additional evaluation to explore the transferability of prediction models between genetically distinct populations. In this study, samples with high GEBVs predicted by both the BB and GBLUP models in the nF0_TT population exhibited higher survival rates at the end of the thermal challenge experiment (Fig. 10). However, moderate differences were observed between the predicted GEBVs obtained through k-fold cross-validation within the dF0_TT population and cross-validation using the nF0_TT population (Supplementary File 6).

To investigate the consistency of genomic predictions across populations, we compared GEBVs for nF0 individuals generated using two training datasets: nF0 (within-population prediction) and dF0 (across-population prediction). Comparisons were conducted separately for DPC_Date and DPC_Time to determine whether predictive patterns were consistent across these related TT traits. Fig. 10 shows scatterplots of GEBVs from the two prediction scenarios for the same nF0 fish, with revised axis labels indicating the prediction source population. The clustering of points along the 1:1 line indicates the degree of agreement between within- and across-population predictions.

To further evaluate model performance, the 100 individuals with the highest GEBVs predicted by each model (BB and GBLUP) were compared to actual survival outcomes in the nF0_TT population. Notably, 94 % of the individuals identified by the BB model as having high GEBVs survived, compared to only 46 % of those identified by the GBLUP model (Supplementary File 7). This indicates that the BB model provides a more accurate prediction of survival under thermal stress conditions.

4. Discussion

Global warming poses notable challenges to the sustainability and productivity of aquaculture due to increasing water temperatures, which disrupt the growth, reproduction, and overall health of aquatic species that are adapted to specific thermal ranges (Islam et al., 2019).

Genomic prediction has emerged as a powerful tool to improve breeding programs by estimating genomic breeding values for traits such as temperature tolerance, disease resistance, and environmental adaptability, using genome-wide markers rather than relying on identifying individual trait-associated markers (Pryce and Haile-Mariam, 2020). By selectively breeding individuals with favorable genetic traits, populations that are better equipped to withstand the adverse effects of global warming can be developed. While our previous study

Table 3
Common SNPs bearing genes for both dF0_TT and nF0_TT populations.

No	Common ID	Gene name	Symbol
1	AX−419312234	Myosin heavy chain, fast skeletal muscle-like	myhc
2	AX−419312236	NLR family CARD domain containing 5	nlrc5
3	AX−419305596	Cerebellin 1 precursor	cbln1
4	AX−419194856	HYDIN, axonemal central pair apparatus protein	hydin
5	AX−419197087	Monocarboxylate transporter 13-like	mtc3
6	AX−419238898	Potassium voltage-gated channel subfamily H member 2-like	kcnc2
7	AX−419194862	Bardet-Biedl syndrome 2	bbs2
8	AX−419311974	Protein serine kinase H1	pskh1
9	AX−419312238	Glucose-fructose oxidoreductase domain-containing protein 2	gfoda2
10	AX−419194853	ST3 beta-galactoside alpha−2,3-sialyltransferase 2	st3gal2
11	AX−419194860	Rho GTPase-activating protein 12	arhgap12
12	AX−419236852	Glucose-fructose oxidoreductase domain-containing protein 1	gfoda1
13	AX−419194938	Dihydrofolate reductase-like	dhfr2
14	AX−419311042	Synaptotagmin−2-like	sytl4
15	AX−419310955	NEDD4 binding protein 1	n4bp1
16	AX−419149160	Neuropilin 1	nrp1
17	AX−419197155	Dual specificity tyrosine-phosphorylation-regulated kinase 4-like	dyrk2
18	AX−177864109	Zinc finger protein 423-like	znf423
19	AX−419197419	Purine nucleoside phosphorylase-like	pnp
20	AX−419285770	Serine/threonine-protein kinase	brsk2
21	AX−419311001	Coiled-coil domain containing 33	ccdc33
22	AX−419149141	E3 ubiquitin-protein ligase Siah1	Siah1
23	AX−419292800	SLIT-ROBO Rho GTPase activating protein 1	srgap1
24	AX−419197408	Calcium voltage-gated channel auxiliary subunit beta 2	cacnb2
25	AX−419197051	C-factor-like	C-factor
26	AX−419311414	Ras association domain-containing protein 8-like	rassf8
27	AX−419236846	Peroxisomal membrane protein 11A-like	pex11a

(Udayantha et al., 2023) characterized the genetic architecture of TT in olive flounder via GWAS, validation of significant SNPs across independent populations and systematic evaluation of genomic prediction models for TT remain limited in this species. The present study addresses this gap by combining cross-population SNP validation with genomic prediction model assessment.

Heritability, defined as the proportion of phenotypic variation attributable to genetic differences among individuals (Bennett et al., 2014), is a crucial metric for understanding and managing the response of aquatic organisms to climate change. Despite its importance, limited research has focused on the heritability of TT in aquaculture species. Furthermore, existing studies have employed diverse phenotypic definitions of TT, making it essential to consider these differences for valid cross-study comparisons. In Atlantic salmon (*Salmo salar*), TT was measured as the time to loss of equilibrium during acute thermal stress challenges, yielding a heritability of 0.47 (Benfey et al., 2022). In zebrafish (*Danio rerio*), the heritability of critical thermal maximum (CTmax), defined as the temperature at which fish lose equilibrium, was 0.24 and 0.10 under optimal and high-temperature acclimation, respectively (Morgan et al., 2020). In rainbow trout (*Oncorhynchus mykiss*), TT was assessed as the time to death under sustained high-temperature exposure, with a reported heritability of 0.41 (Gallardo-Hidalgo et al., 2021). These differing measurement approaches, ranging from binary survival to physiological thresholds, highlight the importance of trait definition in genetic studies of thermal resilience. Bennett et al. further classified heritability as "moderate to high" at 0.5 or above and low at 0.1 or below (Bennett et al., 2014). In our study, we observed relatively high heritability for TT traits in olive flounders, with estimates of 0.72 ± 0.04 for DPC_Date and 0.74 ± 0.04 for DPC_Time, and a moderate heritability of 0.39 ± 0.05 for survival. These findings underscore the strong genetic basis of TT in olive flounders, supporting its improvement through selective breeding. Importantly, genomic selection and MAS provide practical advantages in breeding programs by enabling selection for lethal or hard-to-measure traits, allowing earlier selection decisions, and offering tools to manage inbreeding in the absence of pedigree records.

Population structure plays a crucial role in genetic studies, as it influences the distribution of genetic variation and the identification of genes associated with specific traits (Patterson et al., 2006). Understanding population structure is therefore essential for dissecting the genetic basis of complex traits, such as TT. PCA revealed clear subpopulation clusters, indicating non-random population structure within the dataset. Such genetic stratification can influence both GWAS and genomic prediction accuracy, as models tend to perform better when training and validation individuals share closer genetic relationships. This is consistent with previous studies showing a decline in prediction accuracy when applied across genetically distant clusters (Ajasa et al., 2024). Therefore, while within-cluster prediction is more reliable for operational breeding, cross-cluster prediction should be interpreted with caution unless major QTLs are shared between clusters.

QQ plots are widely used to evaluate whether a dataset conforms to a theoretical distribution. The QQ plots showed a slightly left-skewed distribution ($\lambda < 1$), indicating conservative association statistics rather than genomic inflation. Only a small number of SNPs deviated markedly from the null expectation, corresponding to genome-wide significant loci. Similar patterns of conservative QQ plots have been observed in other GWAS of polygenic traits due to stringent population structure correction (Schork et al., 2013). However, such deflation of test statistics suggests that the GWAS model may be conservative, potentially reducing the risk of false positives but also limiting power to detect true associations. Several factors could contribute to this outcome. First, the inclusion of a genomic relationship matrix (GRM) in the linear mixed model accounts for kinship and population structure, which, while essential for reducing confounding, may also over-correct in datasets with strong relatedness. Second, the analyzed phenotypes, survival under thermal stress and time to death, are complex traits likely influenced by many loci of small effect, consistent with a polygenic architecture. Third, our filtering strategy and stringent quality control (e.g., high MAF thresholds and HWE criteria) may have eliminated informative low-frequency variants, further contributing to signal attenuation. Therefore, future studies with larger, more diverse populations and alternative modeling frameworks may help improve the power and calibration of test statistics while accounting more flexibly for relatedness and complex trait architecture.

Our GWAS identified 204 SNPs significantly associated with TT, with 94.6 % of these located on chromosomes 18 and 19. The two most significant SNPs, AX-419312234 and AX-419312236, exhibited the lowest p-values across all three TT traits (SUR, DPC_Date, and DPC_Time), indicating consistent and strong associations. These SNPs were located in intergenic regions on chromosome 19 but closely flanked functionally relevant genes: AX-419312234 is positioned near the myosin heavy chain gene (mhc), and AX-419312236 is adjacent to NLR family CARD domain-containing 5 (nlrc5). Both genes are known to be involved in immune regulation and cellular stress responses, potentially linking them to thermal adaptation mechanisms (Benko et al., 2010; Liang et al., 2007).

Minor allele frequencies for both SNPs exceeded 0.05, ensuring adequate variability for association analyses. Furthermore, allelic substitution effects indicated significant phenotypic differentiation among genotypes, with individuals carrying favorable alleles showing higher survival rates and delayed time to death under heat stress conditions. These findings highlight the potential utility of these SNPs as robust candidates for marker-assisted selection (MAS) targeting TT in olive flounder.

To further validate these SNPs, we examined their association with TT in an independent population (nF0_TT). The SNPs demonstrated a consistent genotype distribution pattern between the dF0_TT and nF0_TT populations. Although several SNPs were consistently associated

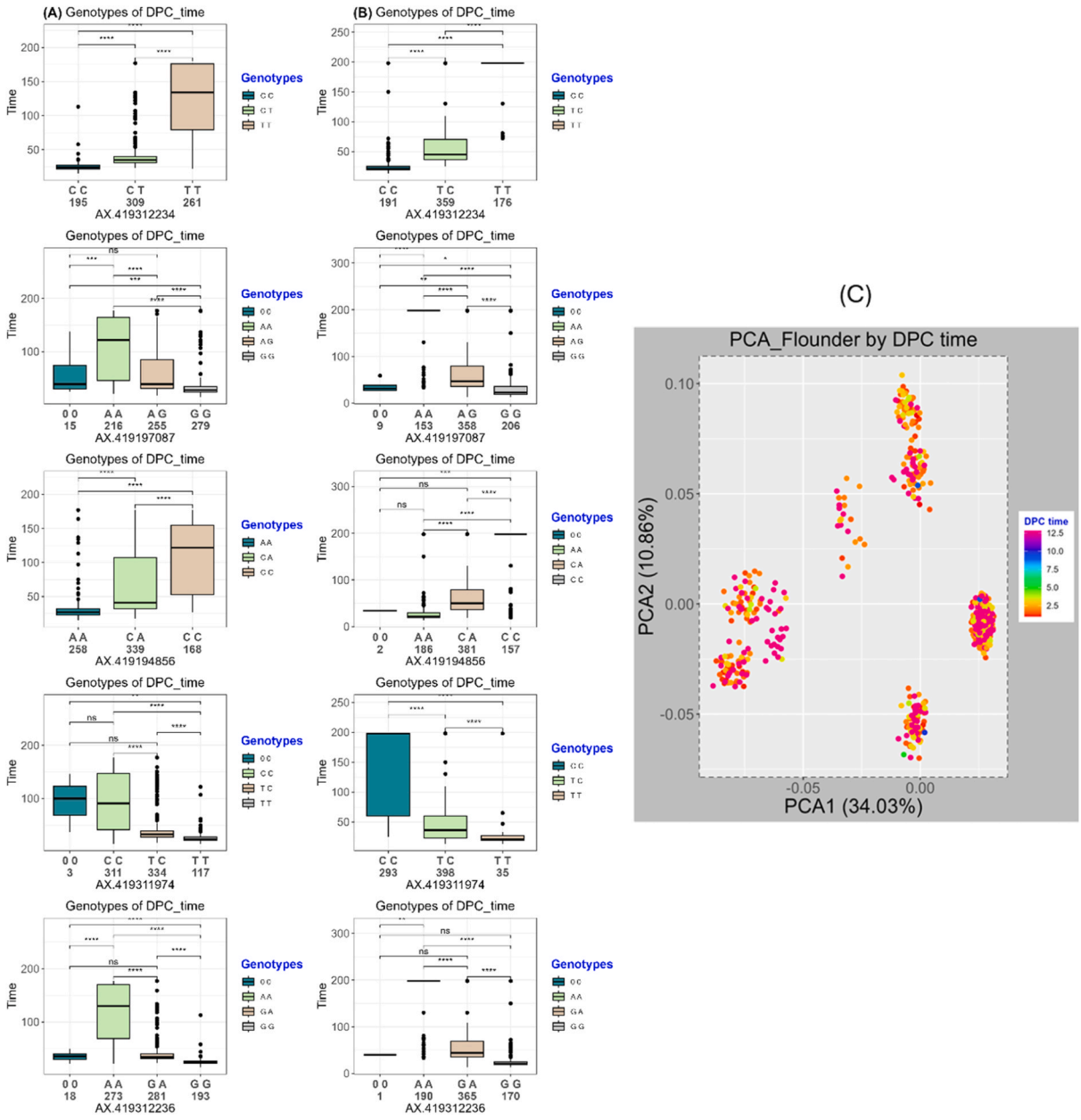

Fig. 6. Validation of the common five genotypes within the top ten phenotypes of (A) dF0_TT and (B) nF0_TT populations for DPC_Time. (C) Principal component analysis plot of the nF0_TT population.

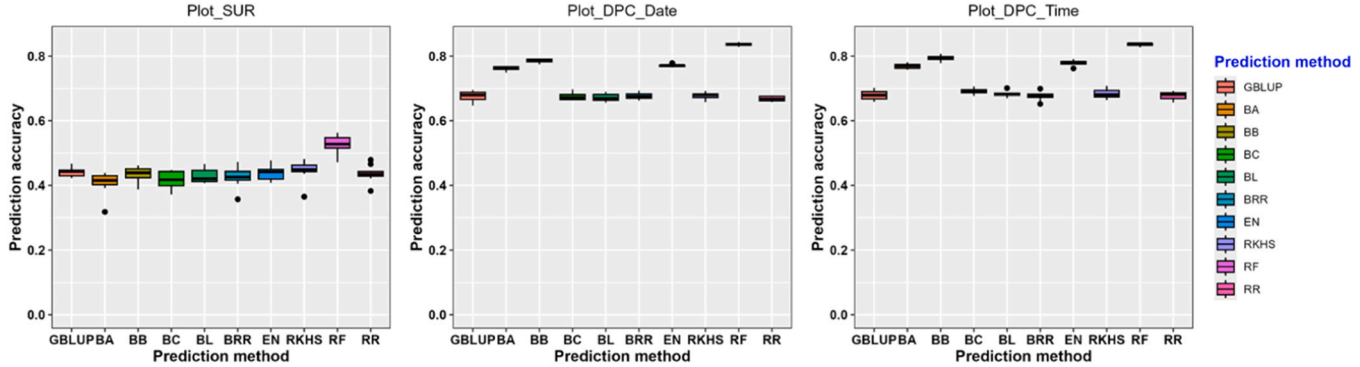

Fig. 7. Comparison of the prediction accuracy of ten different models (GBLUP, BA, BB, BC, BL, BRR, EN, RKHS, RF, and RR) for (A) survival, (B) DPC_Date, and (C) DPC_Time in thermally challenged olive flounders. Prediction accuracies were estimated from k-fold cross-validation using three-fold and ten replicates.

Table 4
Comparison of prediction accuracy of different models; Best Linear Unbiased Prediction (GBLUP), Bayesian A (BA), Bayesian B (BB), Bayesian C (BC), Bayesian L (BL), Bayesian ridge regression (BRR), elastic net (EN), reproductive kernel Hilbert space (RKSH), random forest regression (RF), and ridge regression (RR)) used for thermal tolerance in olive flounders. Data represent the mean ± standard deviation (SD) of 10 replicates.

	GBLUP	BA	BB	BC	BL	BRR	EN	RKHS	RF	RR
dF0_TT_SUR	0.44 ± 0.01	0.41 ± 0.03	0.43 ± 0.04	0.42 ± 0.02	0.43 ± 0.03	0.43 ± 0.02	0.44 ± 0.03	0.45 ± 0.02	0.53 ± 0.03	0.44 ± 0.03
dF0_TT_DPC_date	0.68 ± 0.02	0.76 ± 0.01	0.79 ± 0.01	0.67 ± 0.01	0.67 ± 0.01	0.68 ± 0.01	0.77 ± 0.01	0.68 ± 0.00	0.84 ± 0.01	0.67 ± 0.00
dF0_TT_DPC_time	0.68 ± 0.01	0.77 ± 0.01	0.79 ± 0.01	0.69 ± 0.01	0.68 ± 0.01	0.68 ± 0.01	0.78 ± 0.01	0.68 ± 0.01	0.84 ± 0.01	0.68 ± 0.01

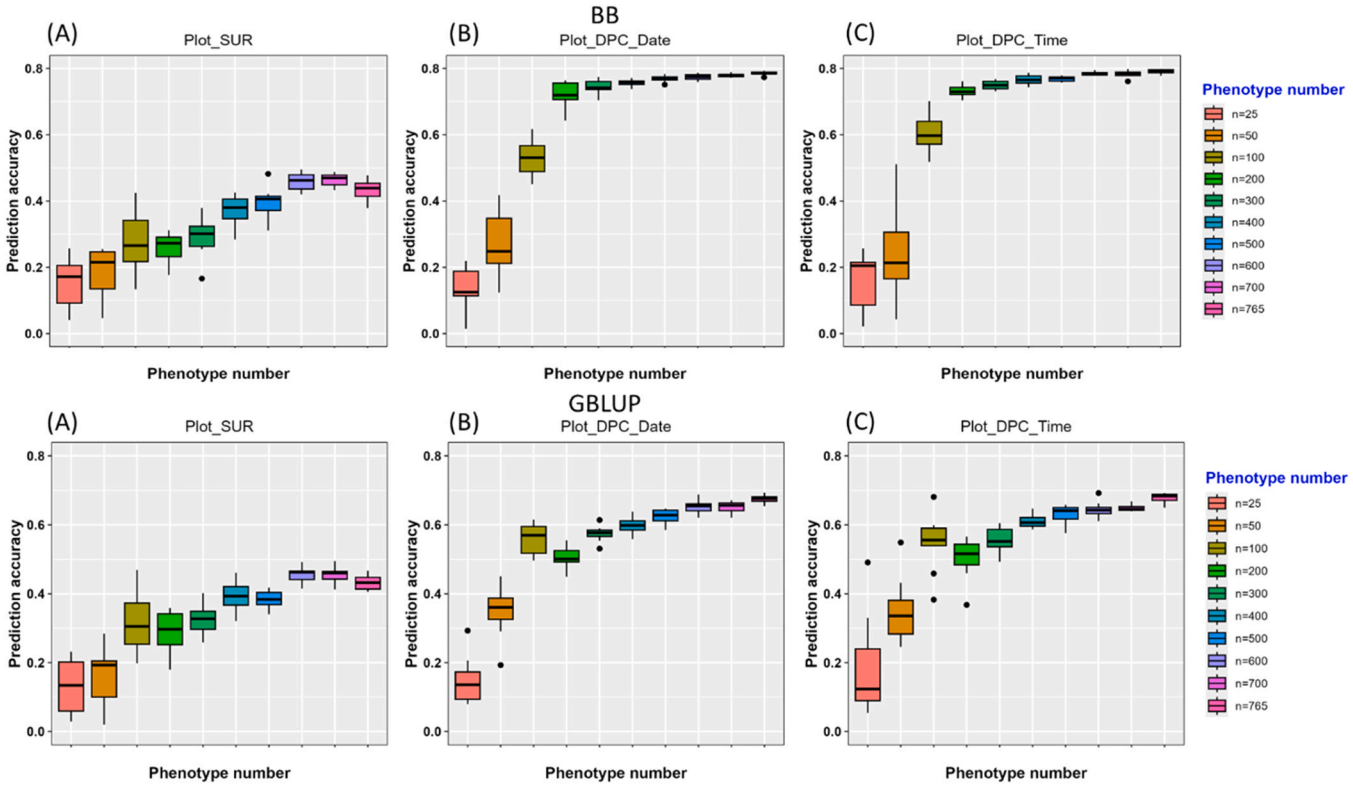

Fig. 8. Prediction accuracies of different population sizes for thermal tolerance-associated phenotype traits of olive flounders. Data are represented as threefold cross-validation with ten replicates for (A) Survival, (B), DPC_Date, and (C) DPC_Time using BB and GBLUP models, respectively.

with TT across populations, their utility for MAS cannot be fully confirmed without quantifying the proportion of phenotypic and genetic variance explained and evaluating genotype-specific differences in TT. Future studies should estimate the effect sizes and variance explained by these loci to assess their true potential for MAS.

Traditional animal breeding has primarily relied on phenotypic selection, where individuals are selected based on observable traits (Zenger et al., 2019). While being effective, this approach is time-intensive and constrained by trait heritability. Genomic selection offers a more efficient alternative by predicting individuals' genetic potential, or GEBVs, for specific traits (Boudry et al., 2021). This technique has transformed aquaculture breeding, enabling the improvement of complex traits, particularly those are difficult or lethal to measure directly, such as disease resistance (Vallejo et al., 2017), feed efficiency (Besson et al., 2019), and environmental adaptation (Ding et al., 2024), while also enhancing progress in more traditionally measurable traits like growth rate (Jerry et al., 2022). Despite its promise, genomic selection for TT in aquaculture remains underexplored. Given the increasing threat of global warming and its adverse effects on aquaculture productivity, strategies to enhance TT in farmed species are urgently needed. In this study, we evaluated both MAS and genomic prediction as strategies to identify olive flounders with high TT. This combined approach leverages the strengths of both methods, enabling precise and efficient selection of thermally-tolerant individuals, thereby enhancing the resilience of olive flounder aquaculture to climate change.

In this study, we evaluated the prediction accuracy of different genomic prediction algorithms for TT in olive flounder. GBLUP and BB were selected as they represent contrasting assumptions about the underlying genetic architecture of traits, while allowing the inclusion of fixed effects that are important for obtaining unbiased prediction estimates. GBLUP assumes an infinitesimal model where all SNPs contribute small, equal effects, making it suitable for traits with highly polygenic control (Karaman et al., 2018). In contrast, BB assumes a sparse genetic architecture, where only a subset of SNPs have large effects, providing better performance when major loci influence the traits (Wolc and Dekkers, 2022). More complex models, such as RF, which showed the highest prediction accuracy, were not used in this step because they cannot explicitly model fixed effects similar to linear mixed models, are less interpretable in terms of SNP effect contributions, and are computationally more demanding for repeated population size evaluations. This strategy aligns with earlier research on genomic selection for TT across species, where BLUP and Bayesian models have been extensively utilized (Dodd et al., 2022; Liu et al., 2022; Yu et al., 2023).

Population size significantly influences prediction accuracy, with larger populations typically yielding higher accuracy (Wang et al., 2022; Yu et al., 2023). Our results confirmed this trend, showing improved prediction accuracy for both the GBLUP and BB models as population

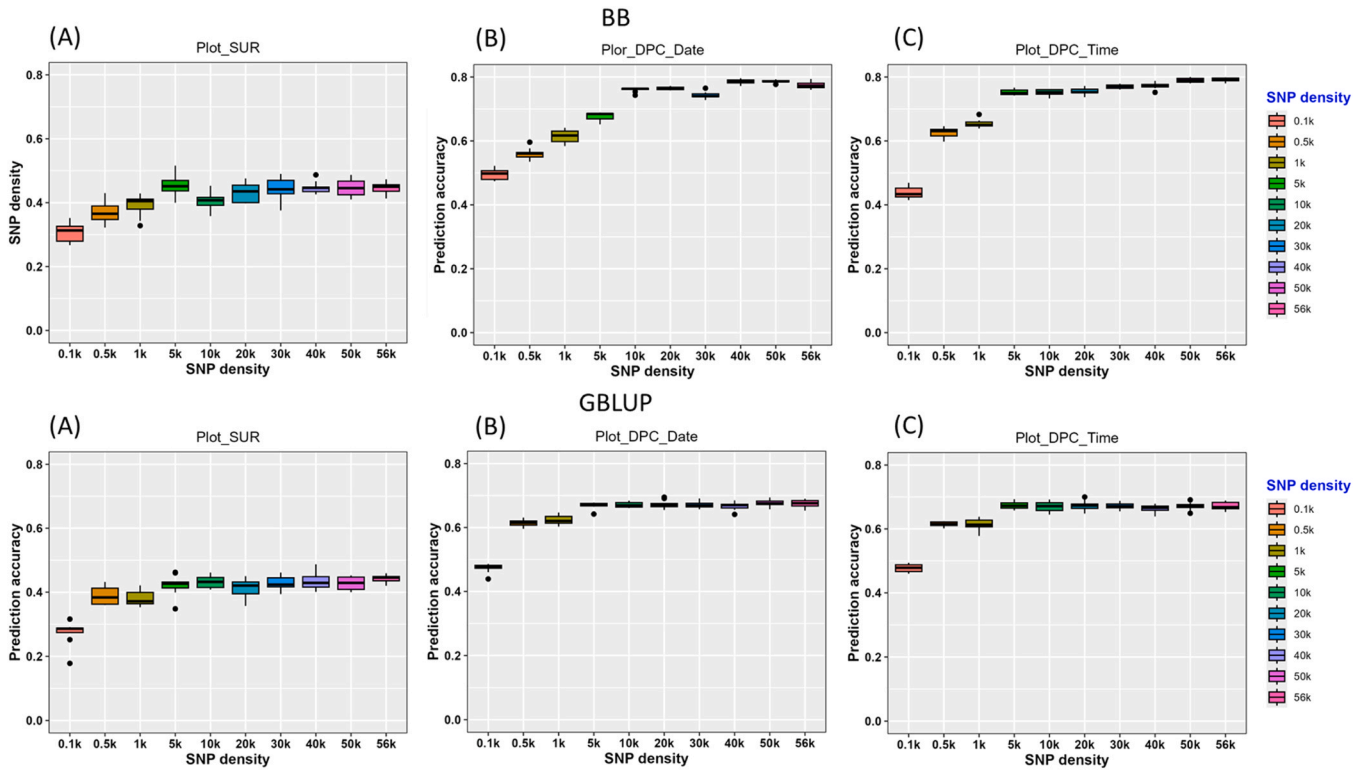

Fig. 9. Prediction accuracies for different SNP densities for thermal tolerance-associated phenotype traits of olive flounders. Data are represented as threefold cross-validation with ten replicates for (A) Survival, (B), DPC_Date, and (C) DPC_Time using BB and GBLUP models, respectively.

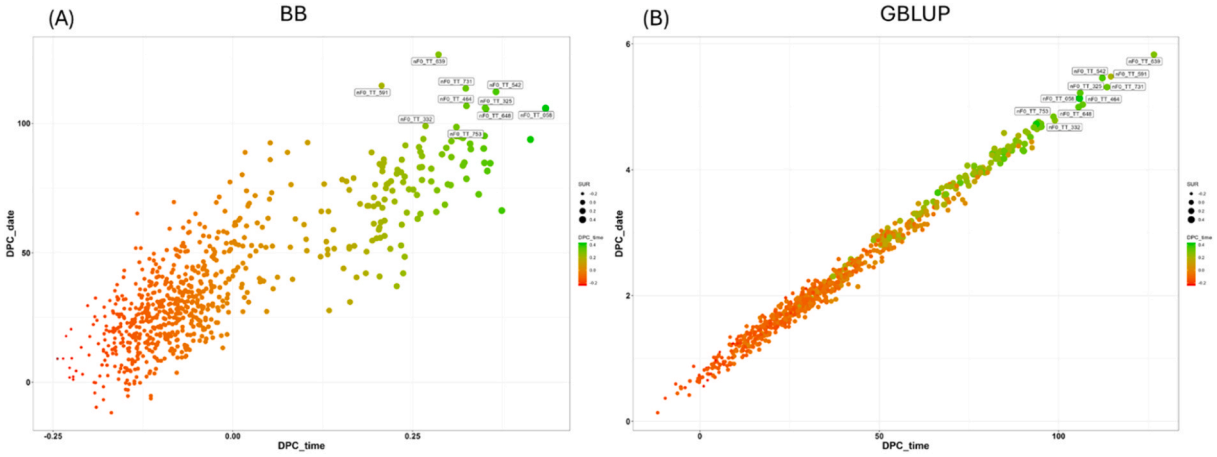

Fig. 10. Scatter plot of cross-validation for nF0_TT population using (A) BB and (B) GBLUP methods. dF0_TT population was used as a training population to predict the genomic estimated breeding values (gEBV) of the nF0_TT population. The highest gEBV values, containing the top ten individuals, are labeled with their IDs.

size increased. Notably, the BB model consistently outperformed GBLUP across all population sizes and for all three TT traits–SUR, DPC_Date, and DPC_Time. This finding suggests that the BB model is particularly robust and effective for smaller datasets, a common constraint in aquaculture breeding programs. Our findings are consistent with prior studies demonstrating the superiority of the BB model over GBLUP for TT prediction in other species, such as the scallop *Chlamys farreri* (Yu et al., 2023). Similarly, a study on growth traits in olive flounder reported higher prediction accuracies with the BB model compared to GBLUP (Omeka et al., 2024). Based on these findings, we recommend the BB model as a preferred tool for genomic prediction of TT in olive flounder, particularly when working with limited population sizes. However, the observed diminishing returns in accuracy beyond lower population size likely reflect the structure of our current dataset, and further validation using larger and more genetically diverse populations is needed to establish robust sample size guidelines for genomic prediction in olive flounder.

We observed that prediction accuracy improved with increasing SNP density, with smaller gains beyond ~5000–10,000 SNPs. This pattern is consistent with previous genomic prediction studies (Wang et al., 2022). Similar results were observed in a study on heat tolerance in abalone (*Haliotis discus hannai*), where prediction accuracies for both GBLUP and BB models plateaued after 5000 SNPs (Liu et al., 2022). Evaluating genomic prediction models requires assessing both accuracy and prediction bias, as biased estimates can undermine selection decisions. Our analysis revealed a trade-off between these metrics. While the RF model achieved the highest accuracy for all TT traits (0.53 for SUR; 0.84 for DPC_Date and DPC_Time), it also produced the most biased predictions,

consistently overestimating GEBVs. In contrast, the BB model offered the best balance of performance, with high accuracy (~0.79 for DPC traits) and almost no prediction bias, making it the most reliable tool for practical selective breeding in this context. Furthermore, we found that training population size was the most critical factor for mitigating bias. Small populations (<200 individuals) produced highly biased and unreliable predictions for both BB and GBLUP models. However, bias stabilized near the ideal value of 1.0 as population size increased, with the BB model achieving this stability with a smaller training set (~200 individuals) than GBLUP (~400 individuals). Conversely, increasing SNP density beyond 5000 markers had little effect on prediction bias, though it did improve accuracy up to a plateau, indicating that investing in a larger training population is more crucial for obtaining reliable GEBVs than simply increasing marker density.

Both the GBLUP and BB models successfully predicted GEBVs for TT in the nF0_TT population. Individuals with higher predicted GEBVs exhibited greater survival rates during the thermal challenge experiment. However, moderate differences in predicted GEBVs were observed between k-fold cross-validation and validation using an independent population, consistent with findings in wheat (Haile et al., 2021). Notably, when comparing survival rates among the top 100 individuals with the highest predicted GEBVs for each model, the BB model demonstrated significantly higher accuracy (94 % survival) compared to the GBLUP model (46 % survival). This performance difference likely reflects the contrasting assumptions underlying the two models: BB assumes a sparse genetic architecture, effectively emphasizing SNPs with large effects, which is particularly advantageous when significant QTLs are shared across populations. In contrast, GBLUP applies an infinitesimal model, distributing effect sizes evenly across all SNPs, which may dilute signals from major loci, especially when training and validation populations differ genetically. These findings underscore the importance of model selection in cross-population genomic prediction and highlight the potential of BB for applications in breeding programs aiming to improve TT in olive flounder.

While our genomic prediction models utilized genome-wide SNP data without prioritizing specific loci, future studies could explore integrating the most significant SNPs identified via GWAS as fixed effects within prediction models.

5. Conclusion

To our knowledge, this is the first study to implement genomic prediction and cross-validation to assess TT in *P. olivaceus*. We identified 204 significant SNPs associated with 141 functional genes, many of which play established roles in thermal stress response. Moreover, validation in an independent population confirmed the association of 35 SNPs with TT, underscoring their potential utility for MAS. Among the evaluated prediction models, the RF and BB models achieved the highest accuracies for predicting TT. While prediction accuracies were variable at lower SNP densities and smaller population sizes, they stabilized when at least 5000 SNPs and 300 individuals were included. Importantly, the BB model outperformed the GBLUP model in cross-validation, particularly for independent populations. Our findings provide a solid foundation for implementing genomic selection strategies, either through MAS, genomic prediction, or a combination of both, to enhance TT in olive flounder breeding programs. This approach is crucial for mitigating the adverse impacts of global warming on olive flounder aquaculture, and such efforts will further enhance the sustainability and productivity of aquaculture in the face of global climate change.

CRediT authorship contribution statement

Sukkyoung Lee: Validation, Investigation, Data curation. **Jihun Lee:** Investigation, Data curation. **Gaeun Kim:** Investigation, Data curation. **Jeongeun Kim:** Writing – review & editing, Project administration, Investigation, Data curation. **H.M.V. Udayantha:** Writing – original draft, Methodology, Investigation, Formal analysis, Conceptualization. **Jehee Lee:** Writing – review & editing, Supervision, Project administration, Funding acquisition. **D.S. Liyanage:** Writing – review & editing, Validation, Supervision, Software. **Dean R. Jerry:** Writing – review & editing. **Cecile Massault:** Writing – review & editing. **David B. Jones:** Writing – review & editing. **Cheong-Uk Park:** Investigation, Data curation.

Author statement

We, the undersigned authors, declare that this manuscript is original and has not been published or submitted elsewhere. All authors have contributed significantly to this work, have reviewed the final version of the manuscript, and approve its submission to the Aquaculture reports. We have disclosed all potential conflicts of interest and confirm that the research was conducted in compliance with ethical standards.

Declaration of Competing Interest

The authors declare that they have no known competing financial interests or personal relationships that could have appeared to influence the work reported in this paper.

Acknowledgment

This research was supported by the Basic Science Research Program of the National Research Foundation of Korea (NRF), funded by the Ministry of Education (RS-2019-NR040078), and the Korea Institute of Marine Science and Technology Promotion (KIMST), funded by the Ministry of Oceans and Fisheries (RS-2022-KS221670).

Appendix A. Supporting information

Supplementary data associated with this article can be found in the online version at doi:10.1016/j.aqrep.2025.103205.

Data availability

Data will be made available on request.

References

Ajasa, A.A., Boison, S.A., Gjøen, H.M., Lillehammer, M., 2024. Accuracy of genomic prediction using multiple Atlantic salmon populations. Genet. Sel. Evol. 56, 38. https://doi.org/10.1186/s12711-024-00907-5.

Alfonso, S., Gesto, M., Sadoul, B., 2021. Temperature increase and its effects on fish stress physiology in the context of global warming. J. Fish. Biol. 98, 1496–1508. https://doi.org/10.1111/jfb.14599.

Barría, A., Benzie, J.A.H., Houston, R.D., De Koning, D.-J., de Verdal, H., 2021. Genomic selection and genome-wide association study for feed-efficiency traits in a farmed nile tilapia (*Oreochromis niloticus*) population. Front Genet 12. https://doi.org/10.3389/fgene.2021.737906.

Benfey, T.J., Gonen, S., Genetics, M., Bartlett, C.B., Garber, A.F., 2022. High heritability for thermal tolerance in Atlantic salmon. Salmo salar. https://doi.org/10.21203/RS.3.RS-2347113/V1.

Benko, S., Magalhaes, J.G., Philpott, D.J., Girardin, S.E., 2010. NLRC5 limits the activation of inflammatory pathways. J. Immunol. 185, 1681–1691. https://doi.org/10.4049/jimmunol.0903900.

Bennett, G.L., Pollak, E.J., Kuehn, L.A., Snelling, W.M., 2014. Breeding: Animals. Proceeding of Encyclopedia of Agriculture and Food Systems. Elsevier, pp. 173–186. https://doi.org/10.1016/B978-0-444-52512-3.00228-X.

Besson, M., Allal, F., Chatain, B., Vergnet, A., Clota, F., Vandeputte, M., 2019. Combining individual phenotypes of feed intake with genomic data to improve feed efficiency in sea bass. Front Genet 10. https://doi.org/10.3389/fgene.2019.00219.

Boudry, P., Allal, F., Aslam, M.L., Bargelloni, L., Bean, T.P., Brard-Fudulea, S., Brieuc, M. S.O., Calboli, F.C.F., Gilbey, J., Haffray, P., Lamy, J.-B., Morvezen, R., Purcell, C., Prodöhl, P.A., Vandeputte, M., Waldbieser, G.C., Sonesson, A.K., Houston, R.D., 2021. Current status and potential of genomic selection to improve selective breeding in the main aquaculture species of international council for the exploration of the sea (ICES) member countries. Aquac. Rep. 20, 100700. https://doi.org/10.1016/j.aqrep.2021.100700.

Breiman, L., 2001. Random forests. Mach. Learn 45, 5–32. https://doi.org/10.1023/A:1010933404324/METRICS.

Chaivichoo, P., Sukhavachana, S., Khumthong, R., Srisapoome, P., Chatchaiphan, S., Na-Nakorn, U., 2023. Genome–wide association study and genomic prediction of growth traits in bighead catfish (*Clarias macrocephalus* Günther, 1864). Aquaculture 562, 738748. https://doi.org/10.1016/j.aquaculture.2022.738748.

Ding, J., Zhang, Y., Li, X., Wang, J., Gao, X., Xiang, Q., Gao, Z., Lan, T., Jia, S., Lu, M., Meng, R., Wang, X., Wu, X., Zhu, J., Shen, W., 2024. Genomic selection for hypoxia tolerance in large yellow croaker. Aquaculture 579, 740212. https://doi.org/10.1016/j.aquaculture.2023.740212.

Dodd, G.R., Gray, K., Huang, Y., Fragomeni, B., 2022. Single-Step GBLUP and GWAS analyses suggests implementation of unweighted two trait approach for heat stress in swine. Animals 12, 388. https://doi.org/10.3390/ani12030388.

Fernando, R.L., Grossman, M., 1989. Marker assisted selection using best linear unbiased prediction. Genet. Sel. Evol. 21, 467–477. https://doi.org/10.1051/gse:19890407.

Forutan, M., Engle, B.N., Chamberlain, A.J., Ross, E.M., Nguyen, L.T., D'Occhio, M.J., Snr, A.C., Kho, E.A., Fordyce, G., Speight, S., Goddard, M.E., Hayes, B.J., 2024. Genome-wide association and expression quantitative trait loci in cattle reveals common genes regulating mammalian fertility. Commun. Biol. 7 (1), 724. https://doi.org/10.1038/s42003-024-06403-2.

Gallardo-Hidalgo, J., Barría, A., Yoshida, G.M., Yáñez, J.M., 2021. Genetics of growth and survival under chronic heat stress and trade-offs with growth- and robustness-related traits in rainbow trout. Aquaculture 531, 735685. https://doi.org/10.1016/j.aquaculture.2020.735685.

Garcia, A., Tsuruta, S., Gao, G., Palti, Y., Lourenco, D., Leeds, T., 2023. Genomic selection models substantially improve the accuracy of genetic merit predictions for fillet yield and body weight in rainbow trout using a multi-trait model and multi-generation progeny testing. Genet. Sel. Evol. 55, 11. https://doi.org/10.1186/s12711-023-00782-6.

Garcia, B.F., Cáceres, P.A., Marín-Nahuelpi, R., Lopez, P., Cichero, D., Ødegård, J., Moen, T., Yáñez, J.M., 2024. Prioritized imputed sequence variants from multi-population GWAS improve prediction accuracy for sea lice count in Atlantic salmon (*Salmo salar*). Aquaculture 581, 740422. https://doi.org/10.1016/j.aquaculture.2023.740422.

Gianola, D., van Kaam, J.B.C.H.M., 2008. Reproducing kernel hilbert spaces regression methods for genomic assisted prediction of quantitative traits. Genetics 178, 2289–2303. https://doi.org/10.1534/genetics.107.084285.

Habier, D., Fernando, R.L., Kizilkaya, K., Garrick, D.J., 2011. Extension of the bayesian alphabet for genomic selection. BMC Bioinforma. 12, 186. https://doi.org/10.1186/1471-2105-12-186.

Haile, T.A., Walkowiak, S., N'Diaye, A., Clarke, J.M., Hucl, P.J., Cuthbert, R.D., Knox, R. E., Pozniak, C.J., 2021. Genomic prediction of agronomic traits in wheat using different models and cross-validation designs. Theor. Appl. Genet. 134, 381–398. https://doi.org/10.1007/s00122-020-03703-z.

Han, P., Yan, W., Liu, X., Wang, X., 2024. Differential environmental-induced heat stresses cause the structural and molecular changes in the spleen of Japanese flounder (*Paralichthys olivaceus*). Aquaculture 581, 740490. https://doi.org/10.1016/j.aquaculture.2023.740490.

Hayes, B.J., Visscher, P.M., Goddard, M.E., 2009. Increased accuracy of artificial selection by using the realized relationship matrix. Genet Res. 91, 47–60. https://doi.org/10.1017/S0016672308009981.

Islam, Md.A., Uddin, Md.H., Uddin, Md.J., Shahjahan, Md, 2019. Temperature changes influenced the growth performance and physiological functions of Thai pangas *Pangasianodon hypophthalmus*. Aquac. Rep. 13, 100179. https://doi.org/10.1016/j.aqrep.2019.100179.

Jerry, D.R., Jones, D.B., Lillehammer, M., Massault, C., Loughnan, S., Cate, H.S., Harrison, P.J., Strugnell, J.M., Zenger, K.R., Robinson, N.A., 2022. Predicted strong genetic gains from the application of genomic selection to improve growth related traits in barramundi (*Lates calcarifer*). Aquaculture 549, 737761. https://doi.org/10.1016/j.aquaculture.2021.737761.

Jung, J.Y., Kim, S., Kim, K., Lee, B.J., Kim, K.W., Han, H.S., 2020. Feed and disease at olive flounder (*Paralichthys olivaceus*) farms in Korea. Fishes 5, 21. https://doi.org/10.3390/fishes5030021.

Karaman, E., Lund, M.S., Anche, M.T., Janss, L., Su, G., 2018. Genomic Prediction Using Multi-trait Weighted GBLUP Accounting for Heterogeneous Variances and Covariances Across the Genome. G3 Genes|Genomes|Genet. 8, 3549–3558. https://doi.org/10.1534/g3.118.200673.

Lee, D.-W., Choi, Y.-U., Park, H.-S., Park, Y.-S., Choi, C.Y., 2022. Effect of low pH and salinity conditions on the antioxidant response and hepatocyte damage in juvenile olive flounder *Paralichthys olivaceus*. Mar. Environ. Res. 175, 105562. https://doi.org/10.1016/j.marenvres.2022.105562.

Lee, H.-J., Lee, J.H., Gondro, C., Koh, Y.J., Lee, S.H., 2023. deepGBLUP: joint deep learning networks and GBLUP framework for accurate genomic prediction of complex traits in Korean native cattle. Genet. Sel. Evol. 55, 56. https://doi.org/10.1186/s12711-023-00825-y.

Lee, K., 2024. Due to mass mortality at high temperaturesLast year'S. Fish. Farming Prod. decreased first Time 5 years. Korea Econ. Dly⟨https://www.hankyung.com/article/202403229543i⟩.

Li, H., Su, G., Jiang, L., Bao, Z., 2017. An efficient unified model for genome-wide association studies and genomic selection. Genet. Sel. Evol. 49. https://doi.org/10.1186/s12711-017-0338-x.

Liang, C.S., Kobiyama, A., Shimizu, A., Sasaki, T., Asakawa, S., Shimizu, N., Watabe, S., 2007. Fast skeletal muscle myosin heavy chain gene cluster of medaka *Oryzias latipes* enrolled in temperature adaptation. Physiol. Genom. 29, 201–214. https://doi.org/10.1152/physiolgenomics.00078.2006.

Liu, J., Peng, W., Yu, F., Shen, Y., Yu, W., Lu, Y., Lin, W., Zhou, M., Huang, Z., Luo, X., You, W., Ke, C., 2022. Genomic selection applications can improve the environmental performance of aquatics: a case study on the heat tolerance of abalone. Evol. Appl. https://doi.org/10.1111/eva.13388.

Liyanage, D.S., Lee, S., Yang, H., Lim, C., Omeka, W.K.M., Sandamalika, W.M.G., Udayantha, H.M.V., Kim, G., Ganeshalingam, S., Jeong, T., Oh, S.R., Won, S.H., Koh, H.B., Kim, M.K., Jones, D.B., Massault, C., Jerry, D.R., Lee, J., 2022. Genome-wide association study of VHSV-resistance trait in *Paralichthys olivaceus*. Fish. Shellfish Immunol. 124, 391–400. https://doi.org/10.1016/j.fsi.2022.04.021.

Maulu, S., Hasimuna, O.J., Haambiya, L.H., Monde, C., Musuka, C.G., Makorwa, T.H., Munganga, B.P., Phiri, K.J., Nsekanabo, J.D.M., 2021. Climate change effects on aquaculture production: sustainability implications, mitigation, and adaptations. Front Sustain Food Syst. 5. https://doi.org/10.3389/fsufs.2021.609097.

Mesbah-Uddin, M., Guldbrandtsen, B., Capitan, A., Lund, M.S., Boichard, D., Sahana, G., 2022. Genome-wide association study with imputed whole-genome sequence variants including large deletions for female fertility in 3 Nordic dairy cattle breeds. J. Dairy Sci. 105 (2), 1298–1313. https://doi.org/10.3168/jds.2021-20655.

Meuwissen, T.H.E., Hayes, B.J., Goddard, M.E., 2001. Prediction of total genetic value using genome-wide dense marker maps. Genetics 157, 1819–1829. https://doi.org/10.1093/genetics/157.4.1819.

Morgan, R., Finnøen, M.H., Jensen, H., Pélabon, C., Jutfelt, F., 2020. Low potential for evolutionary rescue from climate change in a tropical fish. Proc. Natl. Acad. Sci. 117, 33365–33372. https://doi.org/10.1073/pnas.2011419117.

Ogutu, J.O., Schulz-Streeck, T., Piepho, H.-P.,. Ogutu2012_RR and EN.pdf. BMC Proc. https://doi.org/10.1186/1753-6561-6-S2-S10.

Omeka, W.K.M., Liyanage, D.S., Lee, S., Lim, C., Yang, H., Sandamalika, W.M.G., Udayantha, H.M.V., Kim, G., Ganeshalingam, S., Jeong, T., Oh, S.R., Won, S.H., Koh, H.B., Kim, M.K., Jones, D.B., Massault, C., Jerry, D.R., Lee, J., 2022. Genome-wide association study (GWAS) of growth traits in olive flounder (*Paralichthys olivaceus*). Aquaculture 555, 738257. https://doi.org/10.1016/j.aquaculture.2022.738257.

Omeka, W.K.M., Liyanage, D.S., Lee, S., Udayantha, H.M.V., Kim, G., Ganeshalingam, S., Jeong, T., Jones, D.B., Massault, C., Jerry, D.R., Lee, J., 2024. Genomic prediction model optimization for growth traits of olive flounder (*Paralichthys olivaceus*). Aquac. Rep. 36, 102132. https://doi.org/10.1016/j.aqrep.2024.102132.

Palaiokostas, C., Cariou, S., Bestin, A., Bruant, J.-S., Haffray, P., Morin, T., Cabon, J., Allal, F., Vandeputte, M., Houston, R.D., 2018. Genome-wide association and genomic prediction of resistance to viral nervous necrosis in European sea bass (*Dicentrarchus labrax*) using RAD sequencing. Genet. Sel. Evol. 50, 30. https://doi.org/10.1186/s12711-018-0401-2.

Pandit, N.P., Nakamura, M., 1970. Effect of high temperature on survival, growth and feed conversion ratio of Nile Tilapia, *Oreochromis niloticus*. Our Nat. 8, 219–224. https://doi.org/10.3126/on.v8i1.4331.

Park, T., Casella, G., 2008. The Bayesian Lasso. J. Am. Stat. Assoc. 103, 681–686. https://doi.org/10.1198/016214508000000337.

Patterson, N., Price, A.L., Reich, D., 2006. Population Structure and Eigenanalysis. PLoS Genet 2, e190. https://doi.org/10.1371/journal.pgen.0020190.

Pérez, P., de los Campos, G., 2014. Genome-wide regression and prediction with the BGLR statistical package. Genetics 198, 483–495. https://doi.org/10.1534/genetics.114.164442.

Pryce, J.E., Haile-Mariam, M., 2020. Symposium review: genomic selection for reducing environmental impact and adapting to climate change. J. Dairy Sci. 103, 5366–5375. https://doi.org/10.3168/jds.2019-17732.

Schork, A.J., Thompson, W.K., Pham, P., Torkamani, A., Roddey, J.C., Sullivan, P.F., Kelsoe, J.R., O'Donovan, M.C., Furberg, H., Schork, N.J., Andreassen, O.A., Dale, A. M., 2013. All SNPs are not created equal: genome-wide association studies reveal a consistent pattern of enrichment among functionally annotated SNPs. PLoS Genet 9, e1003449. https://doi.org/10.1371/journal.pgen.1003449.

Statistics Korea, 2022. No Title [WWW Document]. Fishery Production Trend Survey. URL https://kosis.kr/search/search.do.

Stieglitz, J.D., Hoenig, R.H., Baggett, J.K., Tudela, C.E., Mathur, S.K., Benetti, D.D., 2021. Advancing production of marine fish in the United States: olive flounder, *Paralichthys olivaceus*, aquaculture. J. World Aquac. Soc. 52, 566–581. https://doi.org/10.1111/jwas.12804.

Udayantha, H.M.V., Lee, S., Liyanage, D.S., Lim, C., Jeong, T., Omeka, W.K.M., Yang, H., Kim, G., Kim, J., Lee, Jihun, Nadarajapillai, K., Ganeshalingam, S., Park, C.-U., Lee, Jiwon, Oh, S.-R., Gong, P., Jang, Y., Hyun, J., Park, A., Koh, H.-B., Kim, M.-K., Jones, D.B., Massault, C., Jerry, D.R., Lee, Jehee, 2023. Identification of candidate variants and genes associated with temperature tolerance in olive flounders by genome-wide association study (GWAS). Aquaculture 576, 739858. https://doi.org/10.1016/j.aquaculture.2023.739858.

Vallejo, R.L., Leeds, T.D., Gao, G., Parsons, J.E., Martin, K.E., Evenhuis, J.P., Fragomeni, B.O., Wiens, G.D., Palti, Y., 2017. Genomic selection models double the accuracy of predicted breeding values for bacterial cold water disease resistance compared to a traditional pedigree-based model in rainbow trout aquaculture. Genet. Sel. Evol. 49, 17. https://doi.org/10.1186/s12711-017-0293-6.

Wang, Y., Ren, Q., Zhao, L., Li, M., Kong, X., Xu, Y., Hu, X., Hu, J., Bao, Z., 2022. Estimating genetic parameters of muscle imaging trait with 2b-RAD SNP markers in Zhikong scallop (*Chlamys farreri*). Aquaculture 549, 737715. https://doi.org/10.1016/j.aquaculture.2021.737715.

Wolc, A., Dekkers, J.C.M., 2022. Application of bayesian genomic prediction methods to genome-wide association analyses. Genet. Sel. Evol. 54, 31. https://doi.org/10.1186/s12711-022-00724-8.

Yang, J., Lee, S.H., Goddard, M.E., Visscher, P.M., 2011. GCTA: a Tool for Genome-wide Complex Trait Analysis. Am. J. Hum. Genet. 88, 76–82. https://doi.org/10.1016/j.ajhg.2010.11.011.

Yazdi Dr, S. khoshnevis, Shakouri Dr, B., 2010. The effects of climate change on aquaculture. Int. J. Environ. Sci. Dev. 1 378–382. https://doi.org/10.7763/IJESD.2010.V1.73.

Yu, H., Sui, M., Yang, Z., Cui, C., Hou, X., Liu, Z., Wang, X., Dong, X., Zhao, A., Wang, Y., Huang, X., Hu, J., Bao, Z., 2023. Deciphering the genetic basis and prediction genomic estimated breeding values of heat tolerance in Zhikong scallop *Chlamys farreri*. Aquaculture 565, 739090. https://doi.org/10.1016/j.aquaculture.2022.739090.

Zeng, J., Herbert, N.A., Lu, W., 2019. Differential coping strategies in response to salinity challenge in olive flounder. Front Physiol. 10. https://doi.org/10.3389/fphys.2019.01378.

Zenger, K.R., Khatkar, M.S., Jones, D.B., Khalilisamani, N., Jerry, D.R., Raadsma, H.W., 2019. Genomic selection in aquaculture: application, limitations and opportunities with special reference to marine shrimp and pearl oysters. Front Genet 9. https://doi.org/10.3389/fgene.2018.00693.